

On the locus formed by the maximum heights of projectile motion with air resistance

H. Hernández-Saldaña*

*Departamento de Ciencias Básicas,
Universidad Autónoma Metropolitana-Azcapotzalco,
Av. San Pablo 180, México 02200 D.F., Mexico.*

(Dated: May 5, 2018)

We present an analysis on the geometrical place formed by the set of maxima of the trajectories of a projectile launched in a media with linear drag. Such a place, the locus of apexes, is written in term of the Lambert W function in polar coordinates, confirming the special role played by this function in the problem. In order to characterize the locus, a study of its curvature is presented in two parameterizations, in terms of the launch angle and in the polar one. The angles of maximum curvature are compared with other important angles in the projectile problem. As an addendum, we find that the synchronous curve in this problem is a circle as in the drag-free case.

I. INTRODUCTION

An amazing characteristic of some old fashion problems is their endurance. The projectile motion is one of them. Being one of the main problems used to teach elementary physics, variations and not well known facts about it appear in the physics literature of the XXI century. A search in the web [1] or in the *Science Citation Index* gives an idea of this fact. Some of the recent studies deal with the problem of air resistance in the projectile motion and its pedagogical character made of it an excellent example to introduce the Lambert W function, a special function.[2] The Lambert W function is involved in many problems of interest for physicist and engineers, from the solution of the jet fuel problem to epidemics[2] or, even, Helium atom eigenfunctions.[3] One of those problems is the solution for the range R in the case that the air resistance has the form $\vec{f} = -mb\vec{v}$. [4, 5]

In this paper we analyze the not well known fact of the geometrical place formed by the maxima of all the projectile trajectories at launch angle α and in the presence of a drag force proportional to the velocity, we shall denote this locus as $\mathcal{C}_m(\varepsilon)$. The resulting locus becomes a Lambert W function of the polar coordinate $r(\theta)$ departing from the origin. This problem raises as a natural continuation from the nice fact that in the drag-free case such a locus is an ellipse[6–8] with an universal eccentricity $e = \sqrt{3}/2$. [6]

The paper is organized as follows. In section II, the set of maxima for projectile trajectories moving under in the presence of air resistance is presented. In section III we find a closed form, in polar coordinates, to express such a geometrical place, \mathcal{C}_m . In section IV we present a numerical calculation of the curvature of \mathcal{C}_m using the polar angle and the launch angle as parameterizations. Additionally, we demonstrate that the synchronous curve is a circle as in the drag-free case in section V. In section VI we conclude.

II. THE PROJECTILE PROBLEM WITH AIR RESISTANCE

Several approximations in order to consider the air resistance exist in the literature, the simplest is the linear case. In such a case the force is given by

$$\vec{F} = -mb\vec{v} - mg\hat{j}, \quad (1)$$

where m is the mass of the projectile and b is the drag coefficient. The units of b are s^{-1} . The velocity components are labeled as $\vec{v} = u\hat{i} + w\hat{j}$, with $u = dx/dt$ and $w = dy/dt$. The solutions for the position and velocity are obtained through direct integration of Eq.(1) yielding

$$x(t) = \frac{u_0}{b} [1 - \exp(-bt)], \quad (2)$$

$$y(t) = \frac{w_0 + g/b}{b} [1 - \exp(-bt)] - gt/b, \quad (3)$$

for the coordinates, and

$$u(t) = u_0 \exp(-bt), \quad (4)$$

$$w(t) = (w_0 + g/b) \exp(-bt) - g/b, \quad (5)$$

for the speeds. We used the initial conditions $x(0) = y(0) = 0$ and $u_0 = V_0 \cos \alpha$ and $w_0 = V_0 \sin \alpha$. Noticing that the terminal speed is g/b in the y axis.

For the same initial speed V_0 these solutions are function of the launch angle α and the locus formed by the apexes is obtained if time is eliminated between the solutions in time in Eqs. (2) and (3), giving the equation

$$y(x) = \frac{w_0 + g/b}{u_0} x - \frac{g}{b^2} \ln \left(1 - \frac{bx}{u_0} \right), \quad (6)$$

and considering the value at the maximum, via $dy/dx = 0$. The corresponding solution is

$$\frac{x_m}{\rho} = \cos \alpha \sin \alpha \frac{1}{1 + \varepsilon \sin \alpha}, \quad (7)$$

$$\frac{\varepsilon^2 y_m}{\rho} = \varepsilon \sin \alpha - \ln(1 + \varepsilon \sin \alpha), \quad (8)$$

*Electronic address: hhs@correo.azc.uam.mx

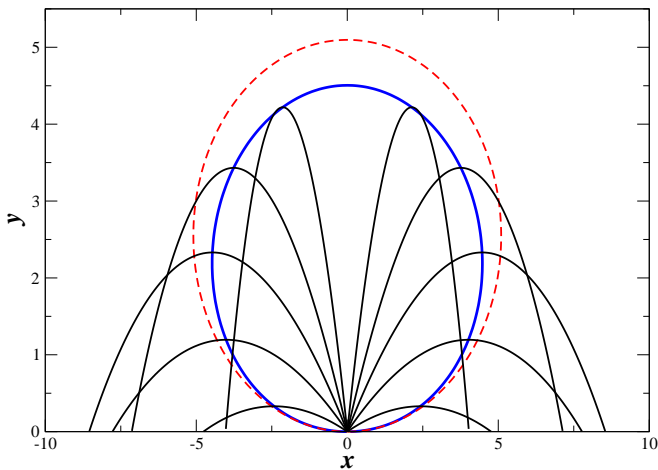


FIG. 1: (color online) Locus $\mathcal{C}_m(\varepsilon)$ formed by the apexes of all the projectile trajectories (continuous line in blue) given by Eqs. (7) and (8) in rectangular coordinates or by Eq. (13), the last one express \mathcal{C}_m in polar coordinates and in term of the Lambert W function. The dashed red line is the ellipse of eccentricity $e = \sqrt{3}/2$ which represents the drag-free case, i.e. $\mathcal{C}_m(0)$. The parameters are $V_0 = 10$ and $\varepsilon = 0.1$.

where we introduce the dimensionless perturbative parameter $\varepsilon \equiv bV_0/g$, the dimensionless length $\rho = V_0^2/g$, and noticing that $\frac{b^2}{g}$ can be expressed as $\frac{\varepsilon^2}{\rho}$. An alternative procedure consists in set the derivative dy/dt to zero to obtain the time of flight to the apex of the trajectory and, evaluate the coordinates at that time. The points (x_m, y_m) conform the locus of apexes $\mathcal{C}_m(\varepsilon)$ for all parabolic trajectories as a function of the launch angle α . In Fig. 1 we plot $\mathcal{C}_m(\varepsilon)$ described by Eqs. (7) and (8), for the drag-free case (in dashed red line) and for $\varepsilon = 0.1$ in continuous blue line. Several projectile trajectories are plotted in thin black lines. The locus of apexes $\mathcal{C}_m(\varepsilon)$ defined by (x_m, y_m) of Eqs. (7) and (8) is described parametrically by the launch angle α and it changes for different values of $\varepsilon \equiv bV_0/g$. In the next section we shall find a description of $\mathcal{C}_m(\varepsilon)$ in terms of polar coordinates and in a closed form using the Lambert W function.

III. THE LOCUS \mathcal{C}_m AS A LAMBERT W FUNCTION

In order to obtain an analytical closed form of the locus we change the variables to polar ones, i.e., $x_m = r_m \cos \theta_m$ and $y_m = r_m \sin \theta_m$. The selection of a description departing from that origin instead of the center or the focus of the ellipse is because the resulting geometrical place is no longer symmetric and the only invariant point is just the launching origin. We substitute the polar forms of x_m and y_m into equations (7) and (8) and

rearranging terms it must be expressed as

$$\frac{r_m(\theta_m)}{\rho} \cos \theta_m \exp\left(-\varepsilon^2 \sin \theta_m \frac{r_m(\theta_m)}{\rho}\right) = \cos \alpha \sin \alpha \exp(-\varepsilon \sin \alpha). \quad (9)$$

The lhs depends on r_m and θ_m meanwhile the rhs depends on α , however the last angle is a function of θ_m and reads as

$$\tan \theta_m = \frac{1}{\varepsilon^2} \frac{(\varepsilon \sin \alpha - \ln(1 + \varepsilon \sin \alpha))}{\cos \alpha \sin \alpha \frac{1}{1 + \varepsilon \sin \alpha}}, \quad (10)$$

by making $\tan \theta_m = y_m/x_m$ from Eqs. (7) and (8).

In order to obtain $\tilde{r}(\theta_m) \equiv r_m(\theta_m)/\rho$ we set

$$f(\alpha(\theta_m)) \equiv \cos \alpha \sin \alpha \exp(-\varepsilon \sin \alpha), \quad (11)$$

since Eq. (10) allows us to have, implicitly, $\alpha(\theta_m)$. We shall return to this point later. Hence, we can write Eq. (9) as

$$-\varepsilon^2 \sin \theta_m \tilde{r}(\theta_m) \exp(-\varepsilon^2 \sin \theta_m \tilde{r}(\theta_m)) = -\varepsilon^2 \tan \theta_m f(\alpha). \quad (12)$$

Where we multiplied both sides of Eq. (9) by $-\varepsilon^2 \sin \theta_m$. Setting $z = -\varepsilon^2 \tan \theta_m f(\alpha)$ and $W(z) = -\varepsilon^2 \sin \theta_m \tilde{r}(\theta_m)$ in Eq. (12), it shall have the familiar Lambert W function form, $z = W(z) \exp(W(z))$, from which we can obtain \tilde{r} as

$$\tilde{r}(\theta_m) = -\frac{1}{\varepsilon^2 \sin \theta_m} W(-\varepsilon^2 \tan \theta_m f(\alpha)). \quad (13)$$

It is important to note that the argument of the Lambert function in this equation is negative for all the values $\varepsilon > 0$. $W(x)$ remains real in the range $x \in [-1/e, 0)$ and have the branches denoted by 0 and -1 . [2] We select the principal branch, 0, since it is the bounded one, however, for values of $\varepsilon > 1.1$ there is a precision problem since the required argument values are near to $-1/e \equiv -\exp(-1)$. It is important to stress that in Eq. (13) the independent variable is the angle θ and, it constitutes the parameterization of the curve \mathcal{C}_m .

The polar expression of \mathcal{C}_m can also be written in terms of the tree function $T(z) = -W(-z)$, giving

$$\tilde{r}(\theta_m) = \frac{1}{\varepsilon^2 \sin \theta_m} T(\varepsilon^2 \tan \theta_m f(\alpha(\theta_m))). \quad (14)$$

We recover the drag-free result

$$\tilde{r} = 2 \frac{\sin \theta_m}{1 + 3 \sin^2 \theta_m} \quad (15)$$

when $\varepsilon \rightarrow 0$. An explanation of this unfamiliar form of an ellipse is given in appendix A followed by a discussion about the $\varepsilon \rightarrow 0$ limit of expression (13) in appendix B.

Formula (13) exhibits the deep relationship between the Lambert W function and the linear drag force projectile problem, since not only the range is given as this function [4, 5]. The problem open the opportunity to study the W function in polar coordinates, that, almost

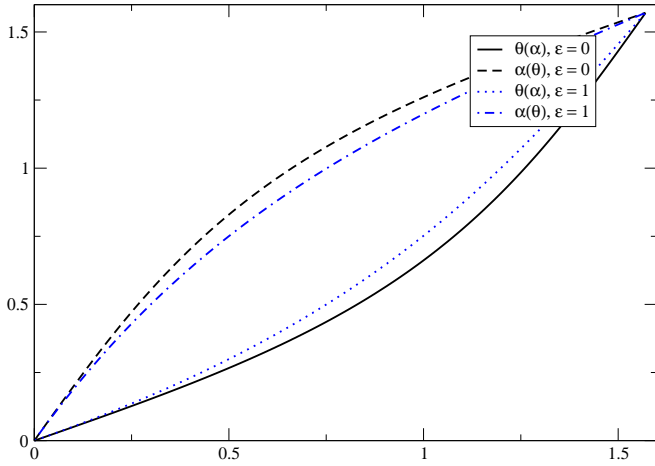


FIG. 2: (color online) The angle θ as a function of the launch angle α for two different values of ε and their inverses.

in the review of reference [2], is absent. Even when it is possible to write the locus in terms of $y_m(x_m)$ this form does not show the formal elegance of relation (13).

Now we return to equation (10) since we need to solve explicitly it in order to have the function $\alpha(\theta_m)$. This task is not trivial since even when we approximate the rhs in expression (10) up to first order in ε ,

$$\tan \theta_m = \frac{\tan \alpha}{2} \left(1 + \frac{\varepsilon}{3} \sin \alpha\right), \quad (16)$$

the inversion is not easy. A way to do the inversion is to expand in a Taylor series the rhs and then invert the series term by term.[9] Using *Mathematica* to perform this procedure up to $\mathcal{O}(18)$, we obtain as a result

$$\alpha(\theta) \approx \arctan(2 \tan \theta) - \frac{1}{3}\varepsilon(2 \tan \theta)^2 + \frac{2}{9}\varepsilon^2(2 \tan \theta)^3 + \frac{1}{54}(27\varepsilon - 10\varepsilon^3)(2 \tan \theta)^4 + \dots \quad (17)$$

The ε -independent terms had been resumated to yield $\arctan(2 \tan \theta)$. However, the series does not converge for values in the argument larger than 1. The reason is the small convergence ratio for the Taylor expansion of $\arcsin(\cdot)$.

An easier way to perform the inversion is to evaluate $\theta_m(\alpha)$ using Eq. (10) and plot the points $(\theta_m(\alpha), \alpha)$, the result is shown in figure 2. The result is in agreement with the plot of Eq. (17) up to its convergence ratio and it is not shown. Notice that this method is exact in the sense that we can obtain as many pair of numbers as we need, a function is, finally, a relation one to one between two sets of real numbers. Another result is to obtain the derivative $d\alpha/d\theta$, since it shall be needed in the following sections. To this end, we note that both functions increase monotonically and their derivatives are not zero, except at the interval end. Hence, we can use the inverse function theorem in order to obtain

$$\frac{d\alpha}{d\theta} = \frac{1}{\frac{d\theta}{d\alpha}}. \quad (18)$$

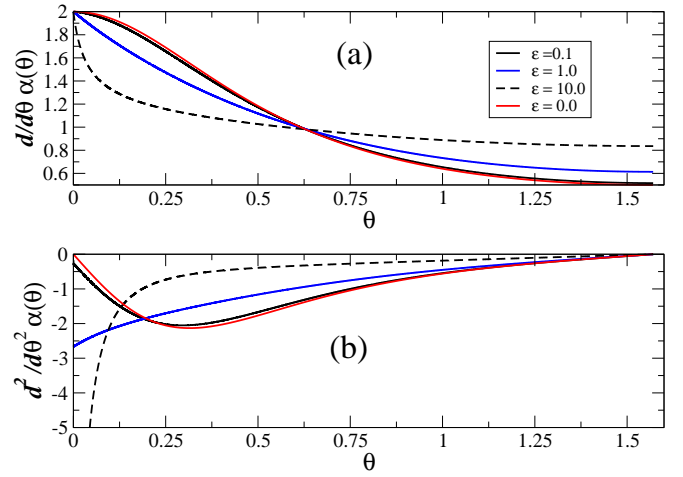


FIG. 3: (color online) (a) First and (b) second derivatives of α as function of θ for various values of parameter ε . Note that major changes occur for $\theta < \pi/4$.

The result is shown in Fig. 3(a) as well as the second derivative in Fig. 3(b). The second derivative is calculated using an approximation to the slope to the function previously calculated and using 10000 points in the interval $[0, \pi/2]$. A smaller number of points could be considered.

IV. THE CURVATURE OF \mathcal{C}_m .

A. Polar angle parameterization.

In the drag-free situation, \mathcal{C}_m is an ellipse and its description is well known, however, in the presence of linear drag this is not the case. We do not expect that the locus could be a conic section and henceforth we need to characterize it. It is usual to consider curvature, radius of curvature or the length of arc in order to characterize a locus. In the present case we consider the curvature of \mathcal{C}_m in both parameterizations, first with the polar angle θ_m and secondly with the launch angle α . We left the calculus of the length of arc to a posterior work, since the calculations became increasingly complex and the goal of the present section is to start the understanding of \mathcal{C}_m and to illustrate the way it can be done using the Lambert W function. Here and in the rest of the section we drop, for clearness, the subindex m in \tilde{r}_m and θ_m .

The corresponding formula for the curvature K for polar coordinates is [10]

$$K = \frac{1}{\rho} \frac{\tilde{r}^2 + 2\tilde{r}_\theta^2 - \tilde{r}\tilde{r}_{\theta\theta}}{(\tilde{r}^2 + \tilde{r}_\theta^2)^{3/2}}, \quad (19)$$

in order to use Eq. (13). Here the subindex θ corresponds a derivative respect to that variable.

A direct calculation on the drag-free $\tilde{r}(\theta)$ of Eq.(15)

yields to

$$K_0 = \frac{1}{2\sqrt{2}\rho} \frac{(5 - 3 \cos 2\theta)^6}{(1 + 3 \sin^2 \theta)^3 (47 - 60 \cos 2\theta + 21 \cos 4\theta)^{3/2}}, \quad (20)$$

which have a maximum at $\theta = 1/2 \arctan(4/3) \approx 0.464$. A graph of this results appears in figure 4 (red line). Note that this value is different from that we obtain if we evaluate $\theta(\alpha = \pi/4) = 1/2$, the launch angle of maximum range. The maximum curvature happens at a smaller angle than the angle of maximum range. It is interesting to note that the angle $2\theta = \arctan(4/3)$ corresponds to a triangle which sides fulfill the relation $3^2 + 4^2 = 5^2$, a Pythagoras' triple.

Using the numerical results for $\alpha(\theta)$ from the previous section, it is possible to carry on the calculation of K (see figure 4) performing the derivatives of \tilde{r} from Eq. (13) in a direct form and evaluating numerically the required values of α and its derivatives. For the required derivatives of $W(z)$ we used the expressions [2]

$$\frac{d}{dx} W(x) = \frac{W(x)}{x(1+W(x))}, \quad (21)$$

and

$$\frac{d^2 W(x)}{dx^2} = \frac{-\exp(-2W(x))(W(x)+2)}{(1+W(x))^3}. \quad (22)$$

Using this method, we obtained good results for values of ε up to ≈ 1 but we require to calculate arguments of the Lambert W function near the limit $z = -1/e$ for larger values of ε . The reliability of our numerical result was done comparing the first and second derivatives of $r(\theta)$ with those corresponding to the ellipse.

As can be seen in figure 4, K present a maximum in all the cases which can be calculated as well. We left to an ulterior work the analysis of the maxima distribution as a function of the perturbative parameter, that is not the case for the curvature with α parameterization as we shall see in the next section.

B. Launch angle parameterization.

For the launch angle parameterization of \mathcal{C}_m we shall use expression [10]

$$\kappa = \frac{x'y'' - y'x''}{(x'^2 + y'^2)^{3/2}}, \quad (23)$$

for calculate the curvature from the rectangular form of equations (7) and (8), where the primes denote derivative respect the parameterization variable, α in this case.

A direct calculation yields

$$\kappa = \frac{\sqrt{2}}{\rho} \frac{\mathcal{P}_1(\alpha)}{(\sqrt{\mathcal{P}_2(\alpha)})^3} \times (1 + \varepsilon \sin \alpha)^2. \quad (24)$$

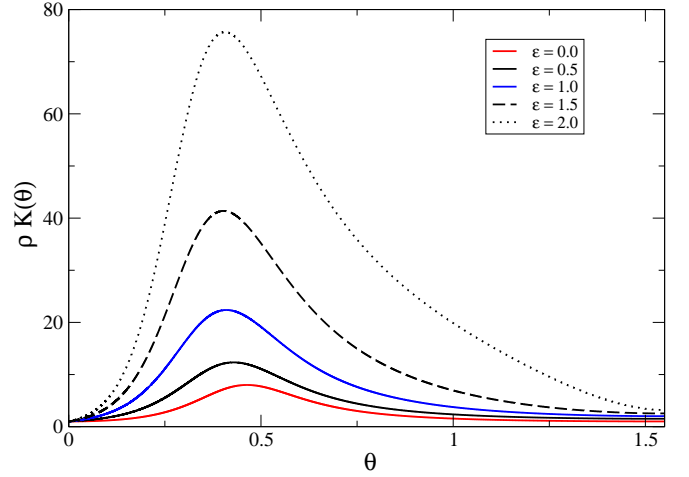


FIG. 4: (color online) Curvature of $\mathcal{C}_m(\varepsilon)$ using the polar angle as the parameter from Eq. (19). In red line appears the corresponding result for the ellipse, Eq. (20). The maximum happens at $\theta = 1/2 \arctan(4/3)$, different from the value of maximum range $\alpha = \pi/4$.

With

$$\mathcal{P}_1(\alpha) = 16 + 6\varepsilon^2 - 8\varepsilon^2 \cos 2\alpha + 2\varepsilon^2 \cos 4\alpha + 30\varepsilon \sin \alpha - \varepsilon \sin 3\alpha + \varepsilon \sin 5\alpha, \quad (25)$$

and

$$\mathcal{P}_2(\alpha) = 5 + 3 \cos 4\alpha + 3\varepsilon^2 - 4\varepsilon^2 \cos 2\alpha + \varepsilon^2 \cos 4\alpha + 10\varepsilon \sin \alpha - 5\varepsilon \sin 3\alpha + \varepsilon \sin 5\alpha. \quad (26)$$

In the limit $\varepsilon \rightarrow 0$, we recover the drag-free curvature

$$\kappa_0 = \frac{16\sqrt{2}}{\rho} \frac{1}{(5 + 3 \cos 4\alpha)^{3/2}}, \quad (27)$$

which have a maximum at $\alpha = \pi/4$ in the interval $\alpha \in [0, \pi/2]$, as expected. A plot of $\rho\kappa(\alpha)$ for several values of ε beginning at zero and ending at $\varepsilon = 10$ appears in Figure 5(a). In red appears the drag-free case. Note that both extremal values increase for increasing ε value as $\rho\kappa(0) \approx (16 + 6\varepsilon - 6\varepsilon^2)$ and $\rho\kappa(\pi/2) \approx \varepsilon$. Notice that for small ε , the κ crosses the drag-free curvature κ_0 .

The angles α^* at which κ attain their maxima are obtained in the usual way and requires to solve, numerical or graphically, the equation

$$3(1 + \varepsilon \sin \alpha^*) \sin 2\alpha^* \times \mathcal{Q}_1(\alpha^*) \mathcal{Q}_2(\alpha^*) + \varepsilon \cos \alpha^* \mathcal{Q}_3(\alpha^*) \mathcal{Q}_4(\alpha^*) = 0, \quad (28)$$

with

$$\mathcal{Q}_1 = 4(3 + \varepsilon^2) \cos 2\alpha^* + \varepsilon(-4\varepsilon - 15 \sin \alpha^* + 5 \sin 3\alpha^*); \quad (29)$$

$$\mathcal{Q}_2 = 16 + 6\varepsilon^2 - 8\varepsilon^2 \cos 2\alpha^* + 2\varepsilon^2 \cos 4\alpha^* + 30\varepsilon \sin \alpha^* - \varepsilon \sin 3\alpha^* + \varepsilon \sin 5\alpha^*; \quad (30)$$

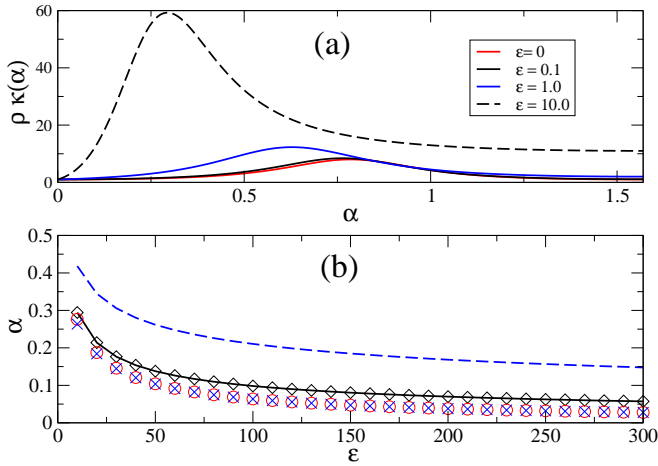


FIG. 5: (color online) (a) Curvature as a function of the launch angle α for increasing values of parameter ε according to equation (24). The values of ε are indicated in the inset. (b) Several important angles as a function of dimensionless parameter ε are plotted. In lines and diamonds appears the angle, α^* , at which the curvature is maximum. In red circles the angle at which the range is maximum according to exact solution, Eq. (34), and in blue crosses the same angle according to Eq. (35) (see text for discussion). In a dashed blue line the angle at which skewness is maximum is plotted.

$$\mathcal{Q}_3 = 5 + 3 \cos 4\alpha^* + 3\varepsilon^2 - 4\varepsilon^2 \cos 2\alpha^* + \varepsilon^2 \cos 4\alpha^* + 10\varepsilon \sin \alpha^* - 5\varepsilon \sin 3\alpha^* + \varepsilon \sin 5\alpha^*; \quad (31)$$

and

$$\mathcal{Q}_4 = 70 + 36\varepsilon^2 - 16(1 + 3\varepsilon^2) \cos 2\alpha^* + 2(5 + 6\varepsilon^2) \cos 4\alpha^* + 154\varepsilon \sin \alpha^* - 31\varepsilon \sin 3\alpha^* + 7\varepsilon \sin 5\alpha^*. \quad (32)$$

In Figure 5(b) the calculated values of α^* as a function of ε appear. This angle is between the optimal angle for maximum range (red circles and blue crosses) and the angle for the greatest forward skew (dashed line).[12]

$$\alpha_{skew} = \arcsin \left[\frac{1}{3\varepsilon} \left((D_+/2)^{1/3} + (D_-/2)^{1/3} - 2 \right) \right], \quad (33)$$

where $D_{\pm} = \pm 3\varepsilon \sqrt{3(27\varepsilon^2 - 32)} + 27\varepsilon^2 - 16$, valid for $\varepsilon > \sqrt{32/27}$. [13] In Figure 5(b) the optimal angles are drawn, in red circles the exact result in terms of Lambert W function[5, 11]

$$\alpha_{max,S} = \arcsin \left[\frac{\varepsilon}{\exp \left(W \left(\frac{\varepsilon^2 - 1}{e} \right) + 1 \right) - 1} \right], \quad (34)$$

and the approximated result[4]

$$\alpha_{max,W} = \frac{W(\varepsilon^2/e)}{\varepsilon}. \quad (35)$$

Both expressions are equivalent for large ε but differ at small ε , as expected.

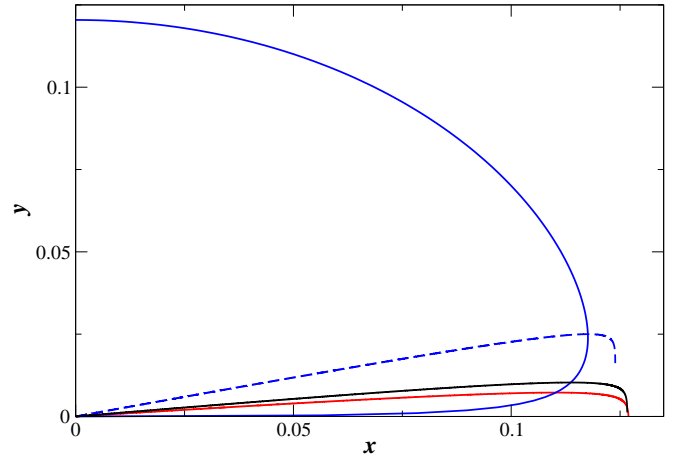


FIG. 6: (color online) Orbits launched at different angles and the corresponding geometrical place $\mathcal{C}_m(\varepsilon)$ for $\varepsilon = 80$. See text for explanation.

Meanwhile the difference between these angles at small perturbative parameter is unimportant, at large ε the behavior of the corresponding trajectories is different. One reason is the large asymmetry in the locus formed by the set of apexes. In Fig. 6(a) we plotted $\mathcal{C}_m(\varepsilon)$ and the corresponding trajectories for the different launch angles for $\varepsilon = 80$. The blue line corresponds to $\mathcal{C}_m(\varepsilon)$, note that the maximum height is $y \sim 0.12$ in contrast to $y \sim 5.0$ for the drag-free case, however, this can be the case of small friction parameter b and large initial velocity V_0 giving a large ε value. In a black line appears the orbit launched at α^* , in red line the corresponding to attain the maximum range and in blue dashed line the orbit with maximum skewness.

V. THE SYNCHRONOUS CURVE

In MacMillan's book[7] the calculation of the synchronous curve was done for the drag-free case. This curve is formed if many projectiles were fired simultaneously from the same point, each one with at different launch angle and same initial speed V_0 . The locus will be a circle of radius $V_0 t$ and center in the point $(0, -\frac{1}{2}gt^2)$, i.e.

$$x^2 + \left(y + \frac{1}{2}gt^2 \right)^2 = V_0^2 t^2. \quad (36)$$

Here, we shall demonstrate that a circle is the synchronous curve in the linear drag case as well. Following reference [7], we eliminate the launch angle α from the position solutions, in the present case they are equations (2) and (3). We write down $\cos \alpha$ and $\sin \alpha$ and rearrange

the terms to give,

$$\cos \alpha = \frac{b}{V_0} \frac{x}{1 - \exp(-b)}, \quad (37)$$

$$\sin \alpha = \frac{b}{V_0} \frac{y - \frac{g}{b^2}(1 - bt - \exp(-bt))}{1 - \exp(-bt)}. \quad (38)$$

Substituting these expressions in the identity $\cos^2 \alpha + \sin^2 \alpha = 1$ we obtain

$$x^2 + (y - y_c(t))^2 = R^2(t). \quad (39)$$

With

$$y_c(t) = \frac{g}{b^2}(1 - bt - \exp(-bt)), \quad (40)$$

the center and

$$R(t) = \frac{V_0}{b}(1 - \exp(-bt)), \quad (41)$$

the radius. In order to recover the case where $b \rightarrow 0$, we consider a Taylor expansion for the exponential up to second order in the exponential in Eq. (40) and up to first order in Eq. (41). The fact that this circle exists in the presence of a drag force is remarkable.

VI. CONCLUSIONS

We obtained an explicit form for the locus \mathcal{C}_m composed by the set of maxima of all the trajectories of a projectile launched at an initial velocity \vec{V}_0 , and in the presence of a linear drag force, $-mb\vec{v}$, i.e. \mathcal{C}_m is the locus of the apexes. In polar coordinates, \mathcal{C}_m is written in terms of the principal branch of the Lambert W function for negative values. This represents the parameterization of the curve by the polar angle θ_m only and gives \mathcal{C}_m in a closed form and exhibits the deep relationship between the Lambert W function and the linear drag problem. The curvature of \mathcal{C}_m was calculated for different values of the dimensionless parameter $\varepsilon \equiv bV_0/g$ in two parameterizations. The first one, the polar parameterization, shows a maximum that slightly departs from the drag-free case in $\theta = 1/2 \arctan(4/3)$. A wider exploration of the functional dependence respect to ε is pending due to numerical accuracy in the calculation of the Lambert W function near the limit at $x = -1/e$. In the case of a parameterization using the launch angle α there is not such a restriction. In this case, the curvature was calculated for a wide range of the parameter ε yielding maximum at angle values larger than those corresponding to maximum range. Comparison with the maximum skewness angle [12] was also done and the difference is larger than the previous one. As an addendum, we demonstrate that the synchronous curve, in this case, is a circle as in the drag-free case.

Acknowledgments

This work was supported by PROMEP 2115/35621. HHS thanks to M. Olivares-Becerril for useful discussions and encouragement.

Appendix A: Polar form of an Ellipse with origin at bottom.

Ellipse canonical form or the polar form with the origin considered in one of the focus are standard knowledge. In the present case, however, we require to consider the origin of coordinates located in the *bottom* of the ellipse, since, in the presence of a drag force, the *launching origin* is the only invariant point when we change the drag force value. To obtain the ellipse form, we depart from the drag-free solutions at the locus of the apexes,

$$x_m = \rho \sin \alpha \cos \alpha, \quad (A1)$$

and

$$y_m = \frac{\rho}{2} \sin^2 \alpha, \quad (A2)$$

being $\rho \equiv \frac{V_0^2}{g}$. With the help of the trigonometric relations $\sin 2\alpha = 2 \sin \alpha \cos \alpha$ and $2 \sin^2 \alpha = 1 - \cos 2\alpha$ we transform the upper equations into

$$\sin 2\alpha = \frac{2x_m}{\rho}, \quad (A3)$$

$$\cos 2\alpha = 1 - \frac{4y_m}{\rho}. \quad (A4)$$

Taking the squares in both expressions, summing them and arranging terms, we arrive to

$$\frac{4r_m}{\rho} \left(\frac{r_m}{\rho} (1 + 3 \sin^2 \theta_m) - 2 \sin \theta_m \right) = 0. \quad (A5)$$

Where we used the polar coordinates $x_m = r_m \cos \theta_m$ and $y_m = r_m \sin \theta_m$. The solutions are $r_m = 0$ and

$$r_m(\theta_m) = \frac{2\rho \sin \theta_m}{1 + 3 \sin^2 \theta_m}. \quad (A6)$$

The second one is the required form for the ellipse.

Appendix B: Drag-free limit for \tilde{r}

In order to obtain the drag-free limit for the locus \mathcal{C}_m given in Equation (13), we note that

$$\tan \theta = (1/2) \tan \alpha \quad (B1)$$

and that $f(\alpha) = \sin \alpha(\theta_m) \cos \alpha(\theta_m)$. The first expression is obtainable from the drag-free solutions Eqs. (A1) and (A2), and the second is obtained by setting $b \rightarrow 0$ in Eq. (11).

The expansion in a power series of the Lambert W function up to first order is just the identity [2] and hence,

$$\begin{aligned}\tilde{r}(\theta_m) &= -\frac{1}{\varepsilon^2 \sin \theta_m} W(-\varepsilon^2 \tan \theta_m f(\alpha)) \\ &\approx -\frac{1}{\varepsilon^2 \sin \theta_m} (-\varepsilon^2 \tan \theta_m f(\alpha)) \\ &= \frac{\sin \alpha \cos \alpha}{\cos \theta_m} \\ &= 2 \sin \theta \frac{\cos^2 \alpha}{\cos^2 \theta_m}.\end{aligned}\quad (\text{B2})$$

Where we used relation (B1) in order to obtain the last

line. Using trigonometric identity $\sec^2 \alpha - \tan^2 \alpha = 1$ and Eq. (B1) we obtain that

$$\frac{\cos^2 \theta_m}{\cos^2 \alpha} = 1 + 3 \sin^2 \theta_m. \quad (\text{B3})$$

Using this result in the expression of \tilde{r} we obtain the desired result, Eq. (15).

-
- [1] See for instance scholar.google.com.
- [2] R.M. Corless, G.H. Gonnet, G.H. Hare, D.E.G. Jeffrey, and D.E. Knuth, "On the Lambert W function", *Adv. in Comp. Mathematics* **5**, 329-359 (1996).
- [3] T.C. Scott, A.Lüchow, D. Bressanini, and J.D. Morgan III, "The Nodal surfaces of Helium atom eigenfunctions", *Phys. Rev. A*, **75**. 060101-060104 (2007).
- [4] R.D.H. Warburton and J. Wang, "Analysis of asymptotic motion with air resistance using the Lambert W function", *Am. J. Phys.* **72**, 1404-1407 (2004).
- [5] E. Packel and D. Yuen, "Projectile motion with resistance and the Lambert function", *Coll. Math. J.* **35**(5), 337-350 (2004).
- [6] J.L. Fernández-Chapou, A.L. Salas-Brito, and C.A. Vargas, "An elliptic property of parabolic trajectories", *Am. J. Phys.* **72**, 1109-1109 (2004).
- [7] W.D. MacMillan, *Theoretical Mechanics: Static and the Dynamics of a Particle* (McGraw-Hill, New York and London, 1927). Reprinted in (Dover, New York, 1958), pp. 249-254.
- [8] G.B. Thomas, M.B. Weir, J. Hass, F.R. Giordano. *Calculus*. 11th Ed. (Addison-Wesley, 2004).
- [9] G.B. Arfken. *Mathematical Methods for physicist*. 5th Ed. (Academic Press, 2000).
- [10] E. Kreyzig. "Principal, Normal, Osculating Circle" in *Differential Geometry*. (Dover, N.Y., 1991). E.W. Wiesstein "Curvature" From MathWorld. <http://mathworld.wolfram.com/Curvature.html>.
- [11] S.M. Steward, "A little introductory and intermediate physics with the Lambert function", *Proc. of the 16th Biennial Congress of the Australian Institute of Physics*. M. Colla ed. Vol 2. pp 194-197. Australian Institute of Physics. Parville, VIC (2005).
- [12] S.M. Steward, "Characteristics of the trajectory of a projectile in a linear resisting medium and the Lambert W function", *Australian Inst. of Physics*. 17th. National Congress 2006. Paper No. WC0035.(2006).
- [13] In Ref. 12, the author comment that for $\varepsilon = 1$ we obtain the special value $\alpha_{skew} = \sin^{-1}(1/\phi)$ with $\phi = (1 + \sqrt{5})/2$, the golden ratio. However, the solution that appears in the article is not longer valid for $\varepsilon = 1$. If the solution corresponds to another real root of the equation this special value corresponds to the case when the initial speed is equal to the limit speed b/g . This makes much more intriguing this fact.